UNIVERSITAT DE BARCELONA

A study of the shortwave schemes in the Weather Research and Forecasting model

Alex Montornès Torrecillas

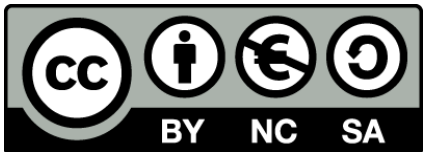

Chapter 4

Description of the sources of error in solar parameterizations

The radiative transfer is an important component of the Earth's atmosphere. However, adding of this physical process in NWP models requires a set of simplifications for two main reasons: i) a full solution of the RTE requires high computational resources, unfeasible with the Central Processing Unit (CPU) power in 1990s and 2000s, and even today with the current computational resources (e.g. Lu et al., 2012; Price et al., 2014) and ii) the radiative variables (i.e. τ, ω_0 and g) are not a solution to the Euler's equations and hence, they must be parameterized as a function of the meteorological fields resolved by the dynamics (e.g. temperature, water vapor) or represented by other physical schemes (e.g. clouds droplets, ice crystals).

Furthermore, while NWP models were not used for solar resource and forecasting applications, the interest on shortwave schemes was limited to drive the day-night patterns within the model (Dudhia, 2014). Under this approach, high accuracy was not really necessary because other components of the model had larger errors and thus, the computational time was prioritized.

With the plane-parallel approximation and assuming horizontal homogeneity (Eq. 2.34), each node of the grid domain can be considered as independent one relative to each other and hence, the RTE is solved in 1-dimensional atmospheric columns. As a consequence, the interaction between columns (e.g. cloud shading) is assumed as a sub-grid scale effect (Eq. 2.155) and it is considered as a second order contribution, sufficient for most of the mesoscale applications with grid resolutions larger than 1 km.

Concurrently, due to the spatial discretization, each grid column is divided into a set of vertical layers assumed as homogeneous. These layers are determined by the model levels in which the resolved and parameterized fields are evaluated. Consequently, the radiative transfer problem boils down to solving the RTE at each layer, including the multiscattering processes between layers at the same column (e.g. adding method). At each layer, the divergence of the upward and downward fluxes determines the heating rate, while the vertically integrated fluxes lead to the surface irradiances, GHI, DHI and DIF.

Moreover, as the model is a simplification of the real atmosphere, the meteorological profiles used as input data for the radiative transfer algorithm are computed with an intrinsic uncertainty, leading to errors in the determination of the fluxes and hence, in the heating rate and the irradiances.

From this description, one can figure out that solar radiative outcomes within NWP models are determined with some degree of error. The importance of these errors depends on the approximations assumed in the simplification of the radiative transfer problem and in the accuracy of the meteorological fields provided by the model. This chapter is divided in two parts, first the different sources of error and uncertainty will be identified and described in Sect. 4. Second, the method that will be used for analyzing the sources of error in the next

chapters will be presented in Sect. 4.2.

4.1 Identification of sources of error

In order to explore the sources of discrepancy between the results of a solar scheme and the real measurements, let us assume the outcome from one specific solar parameterization (e.g. the DHI in New Goddard) given by f at one grid-point and one time-stamp. Additionally, let us assume an analogous observation represented by o.

The difference between f and o defines the accuracy, ϵ, at this node and time-stamp as

$$\epsilon = f - o. \tag{4.1}$$

This deviation is caused by two contributions. On the one hand, the sources of error associated with the approximations necessary for evaluating the radiative transfer described in Chapter 2. On the other hand, the sources of uncertainty in the input meteorological profiles provided by the other modules of the NWP model. Therefore, ϵ can be expressed as

$$\epsilon = \text{error} + \text{uncertainty}. \tag{4.2}$$

The sources of error in turn can be divided in to those that are directly related with the RTE and those that depend upon the vertical settings of the model.

Usually, the vertical resolution is fixed by the number of vertical levels and their distribution from surface to the TOM. As the atmospheric fields vary strongly with height, the layer thickness determines the degree of realism in the assumption of a set of *thin* homogeneous layers composing the atmosphere. Moreover, for most of the meteorological applications, NWP models are configured with a higher density of vertical levels near the surface than in the upper levels and hence, the vertical resolution is not a constant with height. This error can be understood as a *truncation error*, ϵ_{trun}, due to the use of a set of finite atmospheric layers instead of infinitesimal ones.

In direct connection to this, NWP models set a TOM between 50 and 1 hPa, i.e. lower than the TOA, because the upper regions have a negligible impact on the troposphere processes, that are the major interest of the modeling applications. Nevertheless, in radiative terms, it means that a region of the atmosphere is not fully considered in the radiative transfer computation. For example, considering that the surface pressure has an order of magnitude of 10^3 hPa and that TOM is set around 10^1 hPa, about 1% of the atmosphere is not included in the radiative transfer computation. This source of error is named as *TOM error* and it is represented by ϵ_{tom}.

Finally, the set of physical approximations necessary to implement the radiative transfer within NWP models leads to deviations with respect to a *perfect* scheme defining a *physical error* given by ϵ_{phys}.

The sources of uncertainty are associated with the inaccuracy in the determination of the input data used by the solar scheme due to the modeling errors of the other components of the model as well as by the intrinsic unpredictability of the atmosphere. For example, imagine an ideal scheme capable of solving the RTE perfectly, i.e. without the errors described above. Even in this case, an error in the determination of the profile for one of the meteorological fields (e.g. water vapor) would cause unreliable radiative outcomes. Particularly, it could be more dramatic if the NWP model is unable to produce a cloud layer in the correct grid-point with the appropriate characteristics.

Moreover, a solar scheme is not an island within the model. Solar parameterizations interact with the other parts of the model such as the Euler equations or the surface energy balance. Consequently, a bias in the determination of the heating rate or the surface irradiance has an

impact on the results of the other modules, the outputs of whom are used as input fields for the solar scheme in subsequent radiative calls (Montornès et al., 2015e).

This model uncertainty is represented by u_{nwp} and it depends upon many factors, along with high non-linear relationships between the different atmospheric processes represented inside the model.

By expressing Eq. 4.1 as a function of these contributions, we have

$$\epsilon = f - o = \epsilon_{phys} + \epsilon_{trun} + \epsilon_{tom} + u_{nwp}. \tag{4.3}$$

In Sects. 4.1.1 and 4.1.2, ϵ_{phys} and u_{nwp} will be presented in detail, while the truncation and TOM errors are simple concepts that do not need a more detailed discussion for now.

4.1.1 Physical errors

The implementation of the solar radiative transfer within NWP models requires two major approximations as it was discussed in Chapter 2. On the one hand, the complex integro-differential form of the RTE is reduced into a set of non-homogeneous differential equations (Sect. 2.3) expressed as a function of four radiative variables: the optical thickness, the single scattering albedo, the asymmetry factor and, occasionally, the second moment of the phase function. On the other hand, these variables are not a solution of the Euler's equation and hence, they must be parameterized in terms of the meteorological fields provided by the model (Sect. 2.5).

Approximated solution of the RTE

With the exception of Dudhia that uses a simple approach, all schemes discussed in Chapter 3 solve the RTE decomposing the monochromatic intensity in spherical harmonics and expanding the phase function into a number of Legendre polynomials (Eq. 2.32). Usually, solar schemes use the two-stream approximation or one of their variants (e.g. Table 2.1), except FLG that uses the four-stream approach.

The accuracy of these methods has been largely analyzed in many situations for different ranges of the radiative variables and μ_0 as it is studied in several publications such as in Harshvardhan (1986) or Liou (1992), among others. In the book Liou (1992), the author presented a set of experiments comparing the δ-two-stream and δ-four-stream with respect to the discrete ordinate method for a wide range of the most sensitive parameters. Particularly, the optical thickness ranging from 0.1 to 50, ω_0 between 0.3 and 1, and μ_0 from 0 to 1. The asymmetry factor was set to 0.75 in all tests.

In the case of the two-stream approach, the set of conclusions derived from Liou are consistent with Harshvardhan (1986). In all tests, Liou (1992) showed that the δ-four-stream has better skills than the δ-two-stream in the determination of the reflectance as well as the transmittance, in the conservative case (i.e. ω_0=1) as well as in the non-conservative case.

For the conservative case, the reflectance in the δ-two-stream approach was underestimated with an error between 0%, for high τ values, shifting to negative values as τ decreases with a peak of -5% for low τ values. Errors reached values between -20% and -30% when μ_0 is lower than 0.4. The transmittance showed a different behavior being mainly overestimated with a low dependence on τ. For μ_0 larger than 0.5, errors were fitted between -2% and 2% while as μ_0 decreased, the error increased rapidly reaching values around 30%.

The δ-four-stream determined the reflectance with an error between -2% and 1%, with a peak of -10%, for small τ values. The error in the transmittance ranged from 0 to 5%, for any τ, and μ_0, with a maximum around 10% when μ_0 is small.

In the non-conservative case, errors increased considerably, overall in the δ-two-stream approach. In the particular case of ω_0=0.8, errors in the determination of the reflectance fluctuated from -15% to 15% with a high dependence on μ_0. For low τ and μ_0 errors reached

values about -30%. The transmittance showed two different behaviors. On the one hand, for τ higher than 5, the error was mainly a function of τ ranging from -90% (large τ) to 5%. On the other hand, for τ lower than 5, the dependence on μ_0 increased. For large μ_0 values, the error ranged from 1% to 10%, while when μ_0 decreased, it achieved values around 30%.

In the δ-four-stream, the error in the reflectance varied from -5% to 5% with a maximum around -10% being mainly a function of μ_0. The error in the determination of the transmittance showed a low variation with respect to the conservative case.

More recently, Räisänen (2002) presented a revision of different 2-stream algorithms implemented in a NWP model by comparing the results for 24928 columns with the output from a DISORT algorithm composed by 16 streams taken as a baseline. The validation included the analysis of the TOA and surface net shortwave fluxes as well as the total atmospheric column absorption. The mean error considering daytime outcomes in the 2-stream approaches was around 2 Wm^{-2} at surface and between -0.10 and 0.10 Wm^{-2} at the TOA. The total-column absorption had an error around -2 Wm^{-2}. The root mean square error indicated that the PIFM approach is the most accurate method although differences between schemes are relatively low, as it will be confirmed later in this thesis.

Parameterization of the radiative variables

Errors relative to the parameterization of the radiative variables depends on the physical processes described by each scheme (Sect. 2.5 and Chapter 3).

In a clear-sky atmosphere (i.e. without clouds and aerosols), the radiative transfer is reduced to two physical processes: i) the Rayleigh scattering and ii) the absorption due to the molecular gases (i.e. O_3, H_2O and minor gases). Its representation within the solar schemes depends mainly on the spectral division as it is shown in Fig. 3.3.

In virtue of Eqs. 2.109 and 2.140, there are three contributions to the error. First, errors in the determination of the absorption/extinction coefficients. Second, errors in the determination of the mixing ratio of each specie. And, finally, errors in the determination of the dry air mass.

The first kind can be considered as negligible because they are typically measured in laboratories or they are obtained directly from the theory with a high precision. Moreover, the scaling approach described by Eq. 2.121 minimizes the error due to the dependence on pressure and temperature; while methods, such as CKD, reduce the error in these gases in which the absorption has a high dependence on the wavelength, such as it is the case of water vapor.

There are two considerations related to mixing ratios. With the exception of water vapor, all gases are prefixed for each parameterization. Water vapor mixing ratio is an information provided by the NWP model and hence, it is considered as an uncertainty (i.e. u_{nwp}) but not a physical error of the solar scheme.

As ozone is an important gas in terms of radiative transfer in the stratosphere, generally, solar schemes incorporate different ozone profiles as it has seen in Sect. 2.5.1. The spatial and temporal quality of these profiles vary from one scheme to the other as it was shown in Figs. 3.6 and 3.9. Montornès et al. (2015d) analyzed the limitations of these profiles by comparing them with the Multi-Sensor Reanalysis data set during the period 1979–2008 examining the latitudinal, longitudinal and seasonal limitations in the ozone profile specifications of each parameterization. The results indicate that the maximum deviations are over the poles and show prominent longitudinal patterns in the departures due to the lack of representation of the patterns associated with the Brewer–Dobson circulation and the quasi-stationary features forced by the land–sea distribution, respectively. For radiative applications those simplifications introduce spatial and temporal biases with near-zero departures over the tropics throughout the year and increasing poleward with a maximum in the high middle latitudes during the winter of each hemisphere.

Minor gases have a more coarse treatment, with different mixing ratios from one scheme to the other, specially for CO_2 (e.g. 300 ppmv in Goddard vs. 336 ppmv in New Goddard). However, the impact of these gases in the radiative transfer is relatively low and hence, the error introduced by these approximations can be considered as higher order contributions.

Finally, as in the case of H_2O, the dry air mass is also solved by the Euler equations and hence, errors associated to these variables are considered as uncertainties.

Aerosols increase the complexity of the problem. As it has been described in Chapter 3, there are different ways to parameterize the radiative effect of these particles. Some schemes such as CAM or FLG (this one not in the default version as it was discussed in Sect. 3.7) provide background aerosol profiles that are transformed into radiative variables during the scheme execution. Other schemes such as New Goddard and RRTMG work directly with the radiative fields provided externally by the model, via the configuration file or via other models such as WRF-CHEM. Consequently, in schemes such us CAM and FLG, errors due to aerosols can be considered as a physical error because they are included within the parameterization. On the contrary, errors relative to aerosols in New Goddard and RRTMG are external and hence, they are part of the model uncertainty. Authors such as Ruiz-Arias, Dudhia or Lara-Fanego, have been working for a long time on this field with publications such as Ruiz-Arias et al. (2013) or Ruiz-Arias et al. (2014) and several contributions into to the WRF-ARW model. Due to the multiple casuistic of solar schemes as well as the other authors working in this field, this subject will be not developed in this thesis.

In cloudy sky conditions, there are two main factors that can contribute to high errors in the determination of the shortwave fluxes: i) the evaluation of the radiative variables for cloud droplets and ice crystals, and ii) the cloud overlapping approximations and subgrid-scale considerations.

As it was discussed in Sect. 2.5.4, the typical approach for computing τ, ω_0 and g produces reasonable skills. However, the treatment of the cloud overlapping increases the complexity of the problem because it depends on the vertical structure (e.g. cloud fraction).

Cloud composition and features such as cloud droplets mixing ratio, cloud layer thickness or cloud fraction, among others are the most important handicap in the evaluation of the solar fluxes under cloudy conditions.

4.1.2 Model uncertainty

Solar schemes compute the shortwave fluxes by using as vertical profiles the information derived from the other modules of the model. On the one hand, state variables (i.e. temperature, pressure, water vapor and geopotential) are a solution of the Euler equations. On the other hand, physical fields (i.e. cloud droplets mixing ratio, ice crystal mixing ratio and cloud fraction) are parameterized in physical schemes as it was shown in Table 3.1.

An error in the determination of these fields is propagated through the radiative transfer algorithm having a negative effect to the solar skills. Actually, this kind of error is not a limitation of the shortwave parameterization per se, because even in the case of a perfect scheme, the skills would be bad if the other modules work inaccurately. Therefore, from the point of view of a solar scheme, these errors are an uncertainty in the determination of the input data-sets.

In the case of a limited area model, such as the WRF-ARW model is, there are three elements that can produce uncertainty in the determination of the vertical profiles: i) uncertainty in the coarse data-sets propagated during the dynamic downscaling, ii) uncertainty due to the increase of unpredictability with the simulation horizon and iii) uncertainty due to the model simplifications (e.g. phase changes in the microphysics scheme).

The first and second points are two external contributions to the model that can not be controlled easily. For example, if the global model delays the arrival of a cold front, the mesocale model will produce poor results in terms of cloud cover and thus, in the determination

of the solar radiation. The third point allows a deeper discussion that will be important for understanding the methodology presented in Sect. 4.2.

The model resolution determines what scales can be resolved by the model and what scales must be parameterized. The most clear example is the case of cumulus. For coarse resolution grids (i.e. larger than 10 km) the representation of updraft and downdraft as well as subgrid-scale saturation and condensation must be parameterized in denoted cumulus parameterizations (e.g. Tao et al., 2003; Dudhia, 2014). Conversely, for higher resolutions mesoscale models are capable of solving these scales and hence, this parameterization is no longer required. The fact of enabling or disabling this scheme varies the degree of realism in the simulation from a modeling point of view. At the moment of writing this thesis, a similar process is occurring with PBL schemes and its substitution by Large Eddy Simulation (LES) algorithms, leading to reach grid resolutions of hundred of meters in a seamless modeling chain (Montornès et al., 2015a,b,c).

Nevertheless, there are other physical schemes that will be always necessary (e.g. microphysics, radiative transfer) because they represent physical processes that are not included within the Euler equations, as the water phase changes, the land surface processes, etc.

As it is detailed in the WRF-ARW model technical guide (Skamarock et al., 2008), the Euler equations implemented in the model are

$$\partial_t U + (\nabla \mathbf{V} U) + \mu_d \alpha \partial_x p + (\alpha/\alpha_d)\, \partial_\eta p \partial_p \phi = F_U \tag{4.4}$$

$$\partial_t V + (\nabla \mathbf{V} V) + \mu_d \alpha \partial_y p + (\alpha/\alpha_d)\, \partial_\eta p \partial_p \phi = F_V \tag{4.5}$$

$$\partial_t W + (\nabla \mathbf{V} W) - g\left[(\alpha/\alpha_d)\, \partial_\eta p - \mu_d\right] = F_W \tag{4.6}$$

$$\partial_t \theta + (\nabla \mathbf{V} \theta) = F_\theta \tag{4.7}$$

$$\partial_t \mu_d + (\nabla \mathbf{V}) = 0 \tag{4.8}$$

$$\partial_t \phi + \mu_d^{-1}\left[(\mathbf{V} \nabla \phi) - gW\right] = 0 \tag{4.9}$$

$$\partial_t Q_m + (\nabla \mathbf{V} q_m) = F_{Q_m} \tag{4.10}$$

Expressions 4.4, 4.5 and 4.6 are the momentum equations describing the fluid movement, Eq. 4.7 is the energy conservation, Eqs. 4.8 and 4.10 describe the mass conservation for dry air and water vapor, and expression 4.9 is the geopotential equation.

A further description regarding these equations and variables is detailed in the technical guide. However, the interpretation of the left-hand and right-hand parts of these expressions becomes relevant for the following discussion.

The left-hand terms are related with the dynamical and numerical aspects of the model (i.e. those scales higher than the grid resolution). In contrast, the right-hand terms correspond to the unresolved physical processes that need to be parameterized. F_U, F_V and F_W include the friction with the surface, the horizontal and the vertical transport of momentum by turbulent eddies, spherical projections and Earth's rotation. In mesoscale simulations, friction and turbulence mechanisms are modeled by the atmospheric surface layer and PBL schemes/LES algorithms. F_θ is the diabatic heating term in the energy conservation (Eq. 4.7) taking into account the condensation (microphysics scheme), the convection (cumulus scheme), the radiative heating rate (shortwave and longwave schemes) and the heat transport in the boundary layer (PBL scheme). Finally, F_{Q_m} corresponds to the moisture variation due to the precipitation rate, either stratiform (microphysics scheme) or convective (cumulus scheme), due to the evaporation at surface (i.e. LSM) and due to the phase variation during the fall of the hydrometeors (microphysics scheme).

As can be deduced from this discussion, the dynamics and the different physical parameterizations are interrelated by following complex non-linear relationships. Montornès et al. (2015e) analyzed these relationships focusing on the role of the solar schemes and reproduced in Fig. 4.1.

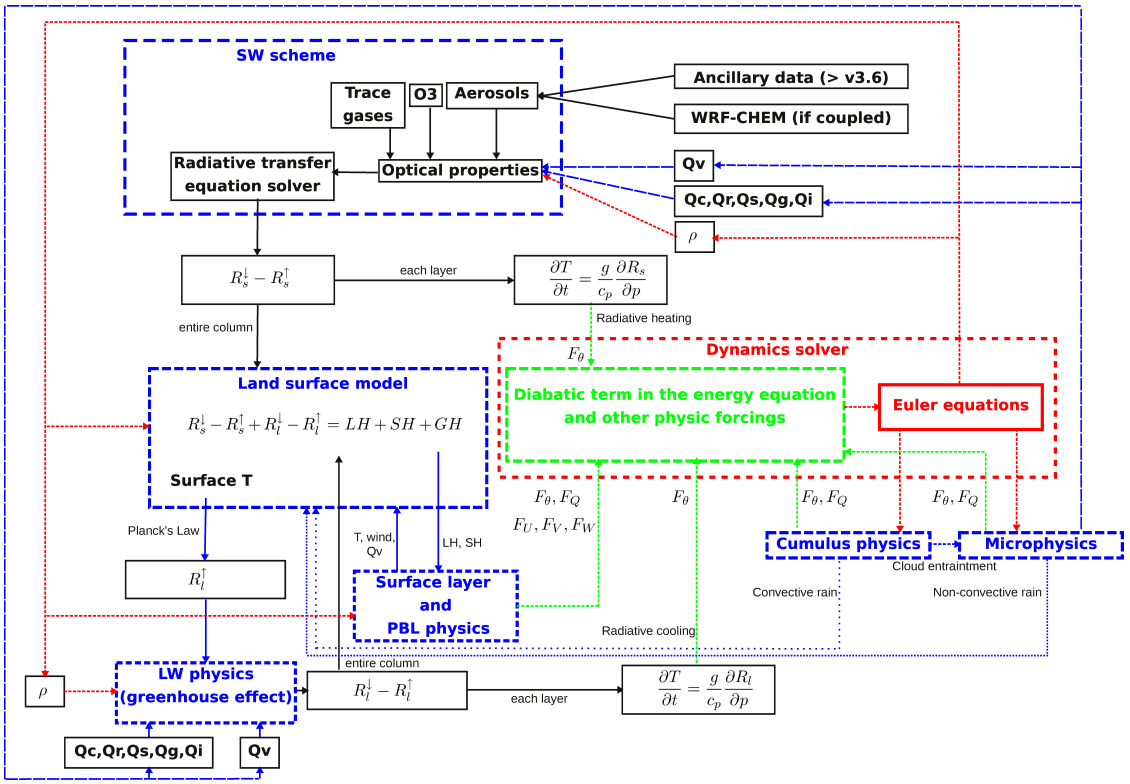

Figure 4.1: Feed-back between different parts of the NWP model focusing on the shortwave scheme. A change on the shortwave scheme is propagated throughout the NWP model following high non-linear relationships. Based on Dudhia (2014) and taken from Montornès et al. (2015e).

Briefly, solar schemes take the incoming profiles derived by the other parts of the model and evaluate the fluxes profiles (upward and downward) at each level. This information is used for computing the heating rate profile at each level as the divergence of the flux (Eq. 2.40).

The heating rate interacts with the Euler equations as a diabatic term in the energy equation (Eq. 4.7). Concurrently, fluxes at surface interacts with the LSM through the surface energy budget and introducing the day cycle to the model (Dudhia, 2014). The importance of this term increases with the simulation horizon because it has a cumulative effect (Montornès et al., 2015e).

The output of the Euler equations in the next time-step is used by the microphysics and cumulus schemes that provide the new cloud properties for the next radiative call. Moreover, these schemes are related with dynamics by F_Q and other physical packages such as the LSM.

Furthermore, the LSM outcomes are important for the atmospheric surface layer and PBL scheme/LES algorithm due to the surface heat fluxes that define the lower boundary conditions for these approaches. Moreover, the skin temperature determined by the LSM defines the Plank's emission in the longwave scheme that at the same time works in a similar way that the shortwave parameterization.

Therefore, one can draw a high degree of complexity from this discussion. Let us recover the example of the *perfect* solar parameterization described previously. As we have discussed, an uncertainty in the determination of the vertical profiles lead to errors in the calculation of upward and downward shortwave fluxes at the different levels composing the atmospheric column. These errors introduce a bias in the heating rate and surface irradiances that is

propagated through the dynamics solver and the LSM, and from there, to the other parts of the model.

As a result, the vertical profiles in the next radiative call will have a higher uncertainty and the error in the shortwave scheme outcomes will increase although originally the parameterization was *perfect*.

Of course, the complexity of the problem increases when a real solar parameterization is considered with the associated errors ϵ_{phys}, ϵ_{trun} and ϵ_{tom}.

This problem was discussed in Montornès et al. (2015e). The paper presents an analysis of the role of the solar schemes on the WRF-ARW model by comparing the effect of four parameterizations (Dudhia, New Goddard, CAM and RRTMG) in two scenarios: i) cloudless and ii) cloudy sky situations for a domain defined over Catalonia (northeast of the Iberian Peninsula). The study shows that the variation of the solar option in identical simulations lead to large differences in the results that increase with the simulation horizon. There are two relevant examples. On the one hand, the simulation with Dudhia is not capable of maintaining the thermal structure of the lower stratosphere provided by the global model because this scheme does not consider the effect of any ozone profile (Sect. 3.3). On the other hand, different solar schemes lead to significant variations on the cloud profiles in the third day-ahead. This problem is illustrated by Fig. 4.2 presented in Montornès et al. (2015e). In this example, two identical simulations were launched with the only difference of the solar parameterization using Dudhia and CAM. Fig. 4.2 shows the vertical profile at a single grid-point located in the middle of the domain for cloud droplets (left-hand) and ice crystals (right-hand). The results correspond to the simulation horizon from 24 to 47 hours ahead with respect to the initialization, i.e. day-ahead. As it can be noted, the cloud composition varies significantly between both simulations. Dudhia produces an important liquid cloud between 3:00 and 6:00 Coordinated Universal Time (UTC), while CAM shifts the cloud for 3 hours with completely different properties in terms of the cloud base and the mixing ratio. Furthermore, Dudhia produces an ice cloud from 18:00 UTC to 21:00 UTC that is missing in the case of CAM.

Henceforth, the analysis of the model uncertainty becomes a titanic work because there are many interrelated factors affecting the results. Furthermore, this kind of analysis does not provide information regarding the accuracy of the solar schemes and their physical limitations. For this reason, u_{nwp} will not be studied in this thesis and it is scheduled as a future work.

4.2 Methodology for evaluating the sources of error

As it has been described in the previous section, differences between f and o have two origins: the sources of error due to the set of approaches assumed by each scheme in the computation of the radiative transfer and the uncertainty associated to the input data for the solar scheme.

The extended methodology for evaluating the skills of a shortwave parameterization is to validate a set of modeled time-series for a given period (e.g. one, two, ten years) by comparing with ground-based station measurements. This procedure can be easily applied to different sites with the purpose of analyzing the optimal configuration of the model at different regions.

Generally, these studies are performed by private companies and the results are cautiously shared in congresses and exhibitions. Nevertheless, some of these tests have been published in peer-reviewed journals. For example, Mathiesen and Kleissl (2011) evaluated the accuracy of the GHI produced by three different NWP models (NAM, GFS and ECMWF) using the Surface Radiation (SURFRAD) network (Augustine et al., 2000) under cloudless and cloudy conditions. Perez et al. (2013) presented three independent validations of the GHI at different sites located in USA, Canada and Europe for different forecasting horizons (from day-ahead to seven days ahead). In this exercise, three NWP models were analyzed: the Canadian Global Environmental Multiscale (GEM) model, ECMWF and several versions of the WRF-ARW model initialized with GFS. More related with the WRF-ARW model, Lara-Fanego et al.

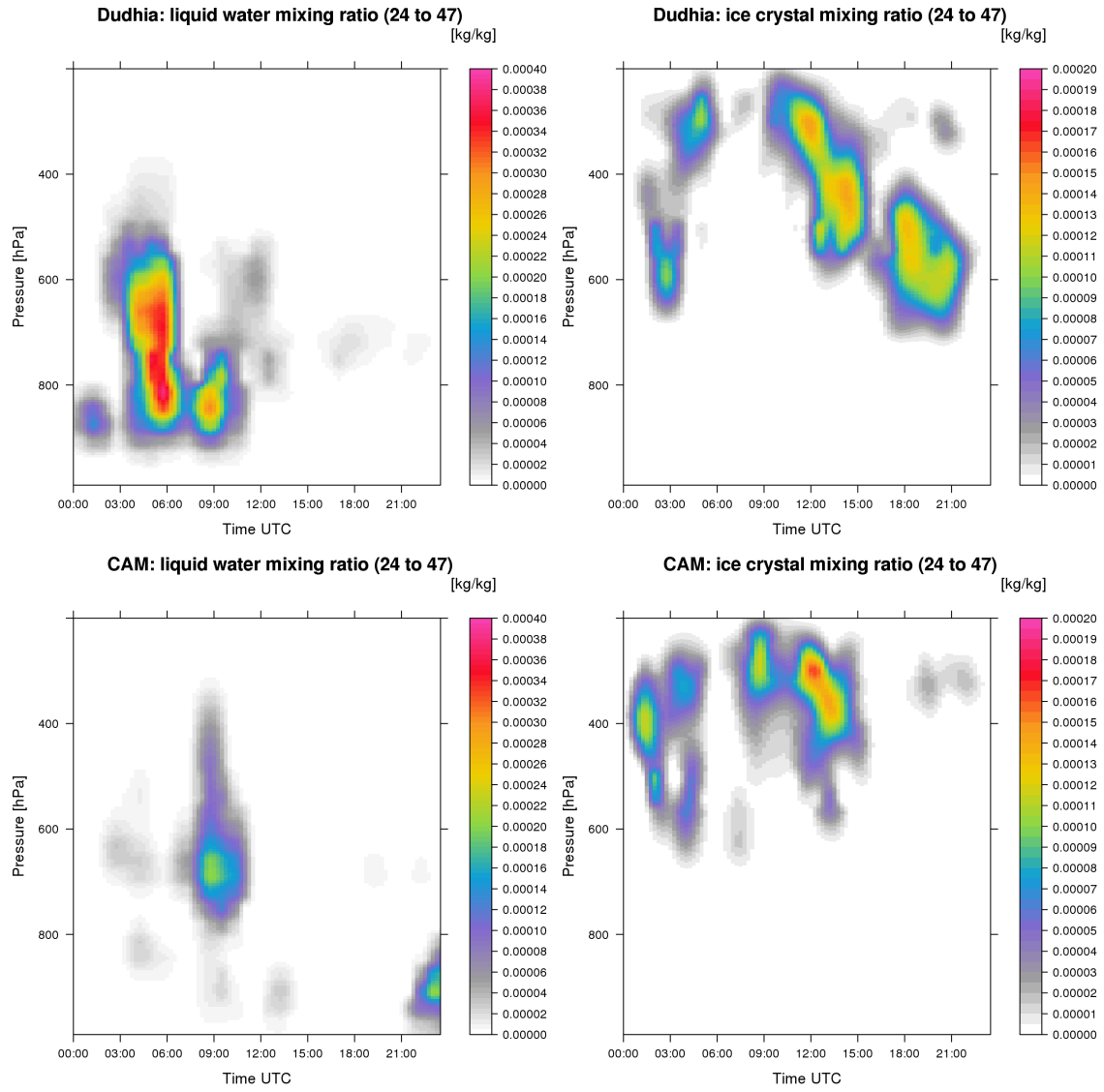

Figure 4.2: Cloud evolution during the day-ahead (i.e. 24-47 h) simulation horizon for Dudhia and CAM, taken from Montornès et al. (2015e).

(2012) validated a post-processed output of GHI and DNI fields with data provided by this model in the three day-ahead forecasting windows at a region located in Andalusia (southern of the Iberian Peninsula) from 2007 to 2008. Ruiz-Arias et al. (2013) examined the ability of two solar schemes in the WRF-ARW model (RRTMG and New Goddard) for modeling the GHI, DNI and DIF fluxes under clear-sky conditions and focused on the aerosol forcing. The outcomes were validated with four sites of the SURFRAD network and one at the Atmospheric Radiation Measurement Central Facility in the CONUS.

This method is a pragmatic approach for obtaining the optimal settings for a solar product, minimizing the errors and/or maximizing the temporal correlation. Nevertheless, this methodology is unsuited to assessing and comparing the skills of different solar parameterizations from a physical point of view because the results are affected by the uncertainty of the model and the interaction of the solar outcomes with the other parts of the model.

In this thesis a different perspective on the issue is presented by ordering the same vertical profile for all schemes. The source code of the solar schemes described in Chapter 3 has been adapted for working with predefined 1-dimensional vertical profiles. These profiles can be provided by ideal conditions or from real soundings as it will be described later.

Under this approach, the input data to the solar parameterizations can be controlled and hence, the uncertainty relative to the model (i.e. u_{nwp}) becomes zero. Consequently, Eq. 4.3 can be written as

$$\epsilon = \epsilon_{trun} + \epsilon_{tom} + \epsilon_{phys}. \tag{4.11}$$

The WRF model has a similar compilation mode called *Single Column Model* (SCM) but it is not exactly the same that the idea of the method required here. WRF-SCM (Wayne, 2015) is a version of the WRF ready to be executed in a 3x3 grid domain in ideal simulations, assuming periodic boundary conditions. The aim of the WRF-SCM is to perform comparison analyses and test physical packages. Nevertheless, this approach is not exactly what it is necessary in the kind of studies that will be discussed in this thesis. On the one hand, this package does not run in a single node. On the other hand, the solar scheme continues interacting with the other modules of the model. Furthermore, as described in Wayne (2015), the WRF-SCM requires a customization of code and script for most of the applications. For this reason, a new tool directly designed to the purposes of the thesis was developed as will be described in Sect. 4.2.1.

4.2.1 Sandbox tool

In the software development jargon, a *sandbox* corresponds to a programming environment in which a specific code is isolated from the main program and tested under different conditions. It represents accurately the main idea behind the set of experiments that will be presented through the following chapters.

The source code of the solar parameterizations is prepared for working with 1-dimensional vertical profiles and on single grid-point and time-stamp. This approach offers the opportunity of testing the shortwave schemes under different scenarios but using the same input data-set in all cases, unlike the experiments with full model real simulations described before.

Conceptually, the code works in a similar manner that the radiation driver described in Sect. 3.2. As it is represented in Fig. 4.3, first of all, the sandbox loads a set of options provided by a file named *file.opt*.

This file includes all settings that varies from one experiment to another. There are five types of information:

- Geographical: coordinates, height above the sea level and surface albedo of the site.
- Temporal: day of the year and UTC time.
- Modeling settings: number of eta levels and TOM value.
- Meteorological: surface pressure and temperature.
- Radiative: physical option (ra_sw_physics) and the parameter swrad_scat, only for Dudhia.

Based on the option ra_sw_physics, the specific information for the selected parameterization is prepared calling the corresponding routine described in Table 3.2.

After that, the astronomical variables are evaluated following the same algorithms than those implemented in the WRF-ARW model and described in Sect. 3.2.1.

In the next step, the input meteorological data is loaded. This information is prepared externally by a set of scripts and stored in a file called *profile.dat*. Concurrently, these scripts work from a set of specifications such as the number of vertical levels and the distribution of the sigma levels. All values for pressure, temperature, air density, geopotential height and mixing ratios for water vapor, ice crystals and cloud droplets are defined at half levels.

With these profiles and the information at surface and TOM provided by the configuration file, the sandbox tool evaluates the fields that are necessary at full levels with a simple interpolation as it is done by the model. Finally, the selected radiative code (Table 3.3) is called emulating the flow of the module_radiation_driver of the WRF-ARW model.

At the moment of starting this thesis, the release of the model was the version 3.4. Thereupon, solar parameterizations were updated progressively until the version 3.8. We updated the sandbox tool accordingly until version 3.6.1. The fact of not continue updating the solar schemes responds to two reasons. The main reason is because at each version, all experiments were repeated with the objective of achieving homogeneity between the different chapters of this document and state-of-the-art outcomes. The other reason is that solar parameterizations in versions 3.7 and 3.8 were not directly affected by large code changes.

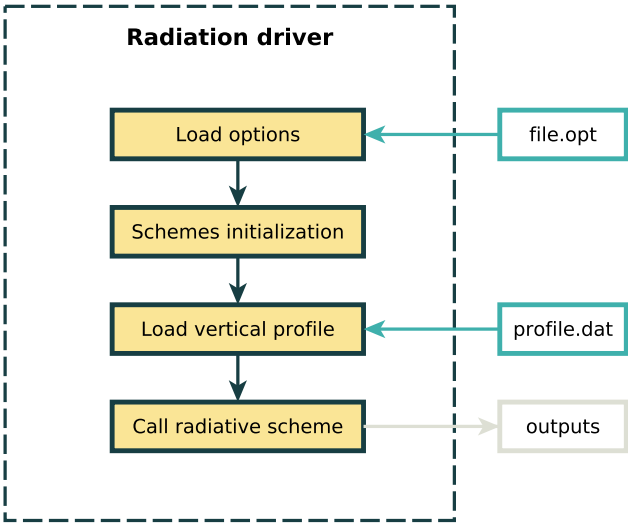

Figure 4.3: Pseudo-flow diagram of the sandbox tool.

Certainly, some of these parameterizations are available directly from the original developers as for example the RRTMG from the AER group. For this reason, some colleagues and other scientists suggested using directly these codes during the development of this thesis. Nevertheless, we decided to use the code provided from the WRF-ARW model for consistency with the solar industry applications in which this mesoscale model is used.

The original code version has been slightly tuned in order to save different outputs necessary for the experiments detailed in the following chapters not available in the versions implemented within the WRF-ARW model. First, all schemes that solve the RTE were adapted for saving the direct and diffuse components of the flux. With the code contribution performed by Dr. Ruiz-Arias in version 3.5.1 and previously described, its code was included in RRTMG and New Goddard. Secondly, parameterizations have been modified for saving other outputs as for example vertical profiles for fluxes: upward, downward direct and downward diffuse. This information is saved in an ASCII file. Finally, in the case of CAM, the aerosols background information has been disabled for a better comparison with the other schemes under the same conditions. In Dudhia, the parameter *swrad_scat* is assumed in the default version, if nothing else is said.

In these schemes such as FLG (Sect. 3.7) with many internal configuration flags (e.g. Tables 3.8 and 3.9), the default settings implemented in WRF are used.